Iranian Journal of Science and Technology, Transactions of Civil Engineering (2024) 48:1903–1915
https://doi.org/10.1007/s40996-023-01301-9

RESEARCH PAPER

Experimental Investigation of the Effects of FRP Bar Fiber Type and Surface Characteristics on the Performance of Reinforced Concrete Beams

Ferhat Aydın[1] · Emine Aydın[1] · Ali Saribiyik[1] · Elif Boru[1] · Şeymanur Arslan[1] · Mehmet Saribiyik[1]

Received: 21 July 2023 / Accepted: 14 November 2023 / Published online: 14 December 2023

Abstract
In this study, experimental investigations were conducted on rectangular cross-section beams to determine the effects of FRP (fiber-reinforced polymer) bars with different fiber and surface characteristics on the flexural performance of reinforced concrete beams. Taking the steel-reinforced beam as a reference, FRP bars were used in the same ratio and spacing in the FRP-reinforced beams. The beams were reinforced with steel rebar and aramid, basalt, glass, carbon FRP bars with sand-coated and ribbed surface characteristics. The effects of FRP bars and bar surfaces on the flexural strengths of the beams and their failure modes were examined through four-point flexural tests. According to the results obtained from the experimental study, the flexural strength of the FRP-reinforced beams nearly has matched that of the steel-reinforced beams. It has been observed that some FRP-reinforced beams with different fiber types and bar surface characteristics showed higher strengths than steel-reinforced beams. While all of the steel-reinforced beams failed only by flexure, the failure modes of the FRP-reinforced beams varied. The fiber type and bar surface characteristics have also influenced the failure modes of the beams.

Keywords FRP bars · Reinforced beams · Flexure · Ribbed surface · Sand-coated surface

1 Introduction

The use of fiber-reinforced polymers (FRP) materials in the construction industry is becoming increasingly common. The properties of FRPs, such as corrosion resistance, lightweight, high tensile strength, low electrical conductivity and not creating electromagnetic fields, have attracted the attention of designers (Aydin 2016; Aydın and Arslan 2021; Hassan and Deifalla 2016; Salem and Deifalla 2022). For these reasons, FRP bars are preferred in structural elements such as bridge decks, marine structures, dock and pier concrete, pavement concrete, ground concrete and concrete sleepers.

In recent years, numerous studies have been conducted on the use of FRP bar instead of steel rebar in concrete structures and the evaluation of their performance (Deifalla 2022; Deifalla and Salem 2022). Experimental investigations have been carried out on the use of steel-FRP hybrid composite bars in beams (Sun et al. 2019), column-beam joints (Qin et al. 2021), blast effects (Johnson et al. 2021), flexural behavior with GFRP bar (Xiao et al. 2021) and behavior in beams produced with sea sand and seawater (Han et al. 2021; Ren et al. 2021; Su et al. 2021; Zhou et al. 2021). Performance studies of hybrid beams using GFRP bar with steel rebar have also been reported (Aydın 2019).

In a study on a model for calculating the shear strength of reinforced concrete beams produced with FRP bars without stirrups (Gao and Zhang 2020), a new model for calculating the shear strength was proposed by analyzing a large number of FRP-reinforced concrete beam experiments. In

✉ Şeymanur Arslan
seymanurarslan@subu.edu.tr

Ferhat Aydın
ferhata@subu.edu.tr

Emine Aydın
emineb@subu.edu.tr

Ali Saribiyik
alisaribiyik@subu.edu.tr

Elif Boru
eorak@subu.edu.tr

Mehmet Saribiyik
mehmets@subu.edu.tr

[1] Department of Civil Engineering, Faculty of Technology, Sakarya University of Applied Sciences, 54050 Sakarya, Turkey

another study (Sogut et al. 2021), experimental results were presented on the effect of transverse and longitudinal FRP bar on the shear behavior of T-beams. Zhang et al. (2021) experimentally determined the flexural behavior of reinforced concrete T-section beams reinforced with FRP bars and investigated analytical flexural strength predictions. Some researchers have experimentally and numerically studied the behavior of basalt FRP-reinforced concrete beams under static and impact loads (Huang et al. 2021). Thermal expansion behavior of FRP bars in concrete (Aydin 2018) and deformations was evaluated. Theoretical studies on the flexural behavior of FRP-reinforced concrete beams have also been carried out (Brózda et al. 2017; Chen et al. 2020; Dhahir et al. 2021; Gravina and Smith 2008; Murad et al. 2021; Yang et al. 2021).

Some studies have been carried out using various fibers in combination with FRP bars in beams. Li et al. (2022) proposed a new model for flexural behavior and flexural design of concrete beams hybrid reinforced with FRP bars and steel fibers. Four-point flexural tests were performed on eleven reinforced concrete beams fabricated with BFRP bars and steel fibers. The failure modes, load–deflection behavior, crack initiation and propagation, service load and ultimate load of the beams were investigated. It was stated that steel fibers can significantly prevent deflection of beams and crack propagation. In another study (Jafarzadeh and Nematzadeh 2020), the flexural behavior of GFRP bar and steel fiber-reinforced high-strength beams after heating was evaluated experimentally and analytically. The beams were exposed to temperatures of 20, 250, 400 and 600 °C and 1% steel fiber was used. Load carrying capacity, load–deflection relationship, number and width of cracks, cracking pattern and ductility of the beams after four-point flexural test were investigated. Liu et al. (2020) investigated flexural cracking in steel fiber-reinforced lightweight aggregate concrete beams with CFRP and GFRP reinforcement. They evaluated the cracking behavior of fourteen plain and steel fiber-reinforced lightweight aggregate concrete beams for two types of FRP reinforcement. Aydın et al. (2021) investigated the effects of FRP reinforcement types and fiber-reinforced concrete on the flexural behavior of hybrid beams. Hybrid beams were formed by placing polypropylene, steel and glass fiber concretes in a GFRP box profile. Flexural tests were performed on each beam type using carbon, aramid, glass, basalt and steel reinforcements in the tension zone. According to the reinforcement types, steel and carbon fiber reinforcement, and steel fiber concrete in fibrous concretes made the most positive contribution to the material behavior. Abdelrahman et al. (2021) investigated the structural performance of beams using both basalt FRP reinforcements and basalt macro-fibers in the beams they produced. A total of 10 reinforced concrete beams of 180 cm length were subjected to five-point loading. As a result of the study, they reported that BFRP-reinforced beams had larger cracks and deformations than steel-reinforced beams. In a similar study (Abushanab et al. 2021), a parametric study including a finite element model was performed using software. Zhu et al. (2018) partially reinforced with steel fiber in FRP-reinforced concrete beams using high-strength concrete. A total of 12 beams were tested using BFRP reinforcement and steel fiber on beams whose flexural performances were examined. Although the addition of steel fibers only in the tension zone reduces the ductility of the beam, they stated that FRP bar-reinforced concrete beams are an effective way to overcome large deflection and large crack width and to reduce the cost.

In an experimental study on the flexural behavior of concrete composite beams reinforced with FRP bars (Ge et al. 2019), the amount, type and thicknesses of bar were used as variables. Some researchers (Dong et al. 2019) suggested using high-strength mortar and corrugated sleeves to evaluate the flexural performance of FRP-reinforced concrete beams. Another study (Sokairge et al. 2022) was conducted to investigate the flexural behavior of reinforced concrete beams reinforced with prestressed near-surface assembly technique using BFRP and GFRP bars. FRP bar type (BFRP and GFRP), reinforcement technique, prestress level were selected as study variables. In a study on prestressed reinforced concrete beams (Atutis et al. 2017), the effects of FRP reinforcement type on shear behavior were investigated, focusing on crack width prediction and shear response analysis of beams. Some researchers (Al-Hamrani and Alnahhal 2021) investigated experimentally and analytically the shear behavior of beams reinforced with BFRP bar and GFRP stirrups. Fourteen beams with BFRP reinforcement, GFRP stirrups and basalt fibers were subjected to four-point flexural tests. Fan et al. (2021) investigated the shear behavior of inorganic polymer concrete beams reinforced with basalt FRP bar and stirrups. BFRP-reinforced inorganic polymer concrete has been proposed as a promising alternative to conventional reinforced concrete to improve the sustainability and durability of structures. It presents a systematic, experimental, theoretical and numerical study of the shear behavior of BFRP-reinforced and stirrup polymer concrete beams. Mehany et al. (2022) used glass and basalt FRP (GFRP and BFRP) bars in lightweight self-compacting concrete beams and investigated the cracking behavior and the bond-dependent coefficient values. Fifteen reinforced concrete beams of 200 mm width, 300 mm height and 3100 mm length were prepared and tested. In the study, concrete density, sand-coated and helical grooved FRP bars, two types of fiber types as GFRP and BFRP bars and longitudinal reinforcement ratio were applied as test variables.

A highly accurate and relatively simple model that can predict the torsional strength of concrete beams reinforced with GFRP stirrups has been proposed by Deifalla et al.

(2014). It was stated that the results of the study showed that further improvements were required in calculating the slope of the diagonal concrete strut and the effective strain in GFRP stirrups. In another study by Deifalla (2015), a model was proposed to predict the full torsional behavior of concrete beams, taking into account parameters such as CFRP or GFRP reinforcements, different cross-section shapes and adhesively bonded FRP stirrups or bent FRP stirrups. In a study, a combined formula was used to estimate the shear strength of FRP-reinforced beams with and without stirrups and the effects of some parameters were examined. As a result of the study, it was determined that shear span and shear reinforcement had a significant effect, while longitudinal reinforcement and modular ratio had less effect (Ebid and Deifalla 2021).

The distinctive aspect of this study lies in its experimental investigations aimed at discerning the impacts of both the fiber type and the surface properties of FRP bars on beam performance. Flexural tests were conducted employing four distinct types of FRP bars on reinforced concrete beams, namely glass fiber-reinforced plastic (GFRP), carbon fiber-reinforced plastic (CFRP), aramid fiber-reinforced plastic (AFRP) and basalt fiber-reinforced plastic (BFRP), each possessing distinct surface properties. Consequently, four different fiber types were utilized in the FRP bars, each featuring two types of surface properties—sand-coated or ribbed surfaces. The results were meticulously analyzed through comparisons with steel-reinforced beams, which were regarded as references, as well as with each other.

The originality of this study is rooted in its comprehensive examination of various FRP bar types and surface characteristics, along with the detailed comparison of their performances against steel-reinforced beams. Such a thorough comparative analysis may hold significance in the construction industry and could impact the utilization of FRP bars in engineering applications.

Table 1 Mechanical properties of steel and FRP bars

Bar type	Strain (%)	Tensile strength (MPa)	Modulus of elasticity (MPa)
Steel	15	600	193,000
AFRP	0.021	1224	58,760
BFRP	0.019	1021	54,700
CFRP	0.011	1304	123,140
GFRP	0.018	883	48,320

2 Experimental Studies

2.1 Mechanical Properties of Materials

The materials used in the production of the beams consist of concrete, steel reinforcement and AFRP, BFRP, CFRP and GFRP reinforcement with different surface properties (sand coated and ribbed) (Fig. 1). While pouring the beam concrete into the molds, five standard cylinder samples were taken and the compressive strength of the concretes was determined after completing the 28-day strength period. As a result of the compressive test, the average compressive strength of the concretes was found to be 26.25 ± 2.7 MPa.

Longitudinal rebar of ϕ10 and stirrup of ϕ8 belonging to S420 strength class were used in steel-reinforced beams. According to the tensile test results, the average yield strength: 467 MPa, tensile strength: 600 MPa and modulus of elasticity: 193,000 MPa were found.

Aramid (AFRP), basalt (BFRP), carbon (CFRP) and glass (GFRP) FRP bars with a ribbed/sand-coated surface of ϕ10 were used as tensile reinforcement in FRP-reinforced beams. GFRP stirrup of ϕ8 was used as shear reinforcement in all FRP-reinforced beams. The behavior and mechanical properties of the bars were determined by tensile tests on steel, AFRP, BFRP, CFRP and GFRP bars. The mechanical

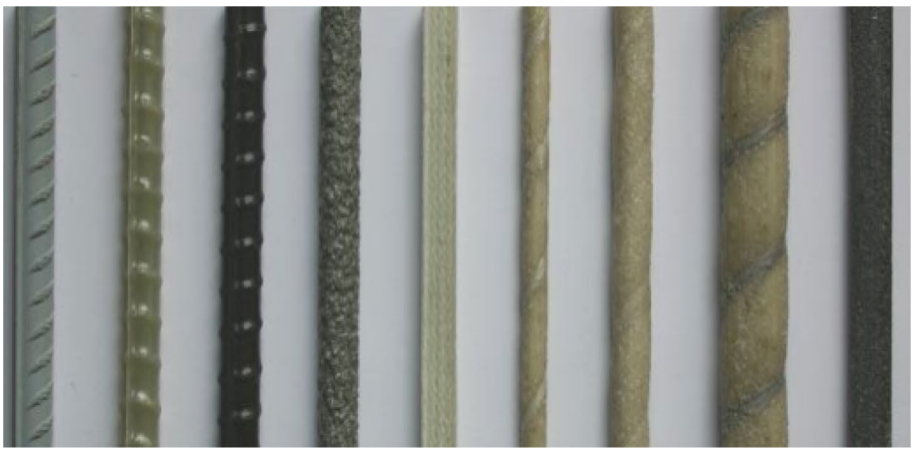

Fig. 1 FRP bars with different surface properties

properties obtained from the test results are presented in Table 1.

2.2 Preparation of Test Specimens

In the tests, a total of twenty-seven beam were produced from ribbed steel reinforcement and AFRP, BFRP, CFRP, GFRP bars, three each with ribbed and sand-coated surfaces. In the experimental study on FRP-reinforced beams, the beams were produced in ½ scale (150 × 250 mm section and 2000 mm length) representing 250/500 mm section and 4000 mm length. According to the Turkish Standards Code (TS 500 2000), the ratio of effective section height (d) to stirrup spacing (s) (d/s) was determined to be 2.25 to prevent shear failure of the reinforced concrete beam, and the longitudinal reinforcement ratio was found to be 0.0093, ensuring that it was above the minimum reinforcement ratio and below the balanced reinforcement ratio. Longitudinal reinforcement of 4ϕ0 was used in the tension zone, and longitudinal reinforcement of 2ϕ10 was used in the compression zone of steel and FRP reinforced beams (Fig. 2). It is aimed that the beam is safe enough in terms of shear by connecting ϕ8 steel stirrups in steel-reinforced beams, ϕ8-ribbed GFRP stirrups in all FRP-reinforced beams and longitudinal reinforcement with 10-cm intervals in the shear zone and 20-cm intervals in the flexural zone. Beam concretes were prepared for flexural tests after curing (Fig. 3).

2.3 Experimental Setup

Beam tests were carried out with a 250 kN capacity four-point flexural test setup. The support span of the beam is 1800 mm, and the distance between loads is 550 mm. The beam is divided into three zones at 625-550-625-mm intervals. The first and third regions are the regions where the flexural moment is low and the shear load is high, and the second region is the region where only the flexural moment is effective. Vertical displacements were measured with displacement meter placed at the lower midpoint of the beam (Fig. 4). The data obtained with the help of data logger and loadcell were transferred to the computer, and load–deflection graphs were drawn.

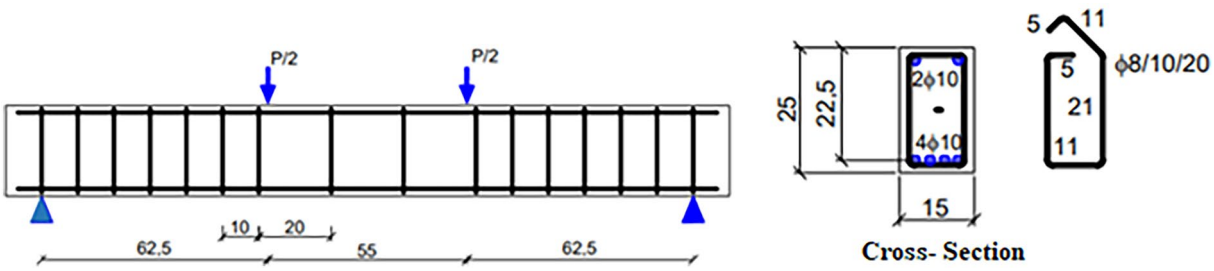

Fig. 2 Beam reinforcement details

Fig. 3 Production of the beams

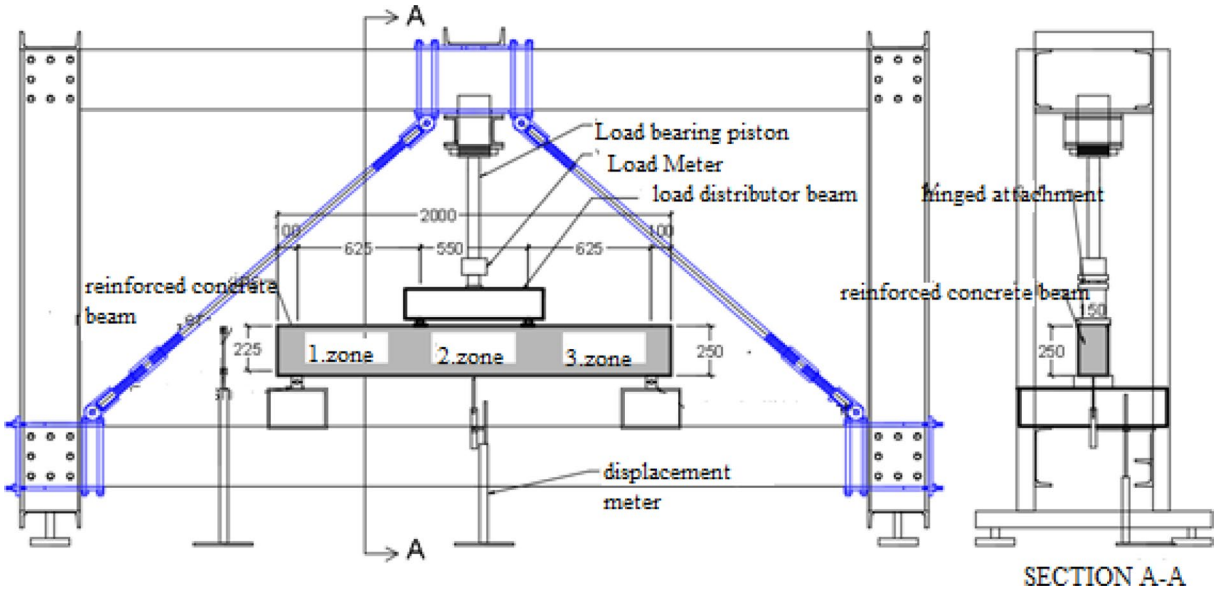

Fig. 4 Flexural frame experimental setup

Table 2 Test results of steel-reinforced beams

Sample	Yield onset		Maximum	
	Load (kN)	Displacement (mm)	Load (kN)	Displacement (mm)
1	112	12.2	122.42	100
2	105	12.5	111.20	100
3	101	12.2	116.51	100
Average	106	12.3	116.71	100
SD	4.55	0.14	4.58	0

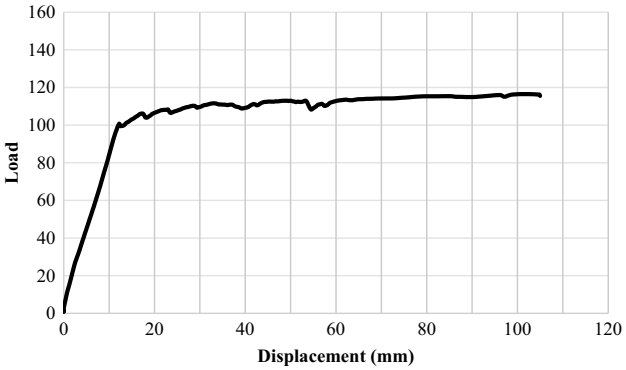

Fig. 5 Flexural test graph of steel-reinforced beams

3 Experimental Results

Four-point flexural test results are presented for steel, AFRP, BFRP, CFRP and GFRP, respectively. In the naming of the test samples, the letter S for the sand-coated surfaces and the letter R for the ribbed ones was used next to the bar type. For example, AFRP_S refers to aramid fiber-reinforced plastic with a sand-coated surface, AFRP_R refers to aramid fiber-reinforced plastic with a ribbed surface.

3.1 Steel-Reinforced Beam Results

Steel-reinforced beams were subjected to a four-point flexural test in the laboratory, and the results were analyzed by transferring the data to the computer. The yield onset and maximum load–displacement values of three steel-reinforced beams are shown in Table 2. Load–displacement graphs representing steel-reinforced beams are given in Fig. 5.

In steel-reinforced beams, the first cracks occurred in the lower region of the beam in the flexural region, and as the loading continued, the cracks progressed toward the upper region of the beam. Steel-reinforced beams showed linear behavior up to the yield load under flexural loading. Beams showed a very ductile behavior after the yield load. All steel-reinforced beams collapsed from the flexural zone (Fig. 6).

3.2 AFRP-Reinforced Beam Results

Concrete cracking and maximum values of AFRP-reinforced beams with sand-coated surface (AFRP_S) and AFRP-reinforced beams with ribbed surface (AFRP_R) are given in

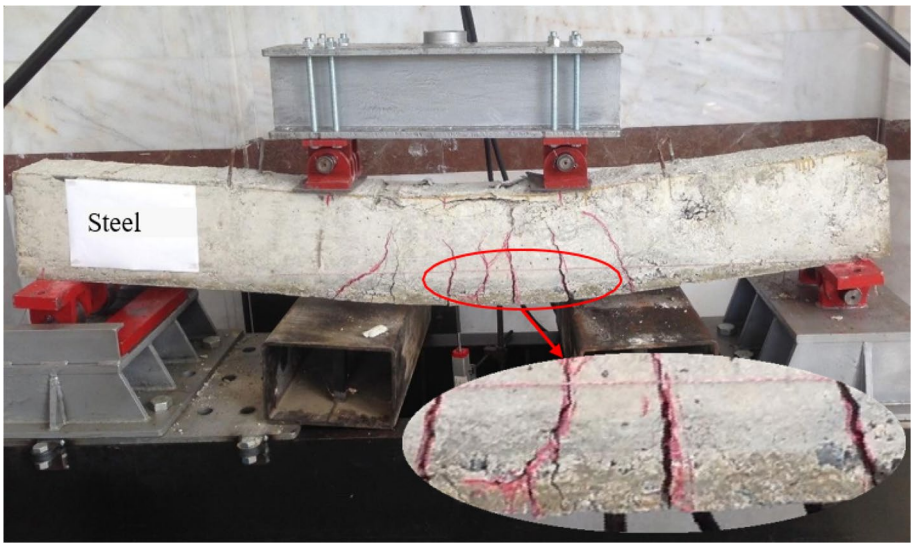

Fig. 6 Steel-reinforced beam deformations

Table 3 AFRP-reinforced beam test results

Beam	Concrete cracking		Maximum	
	Load (kN)	Displacement (mm)	Load (kN)	Displacement (mm)
AFRP_S 1	11.67	1.48	126.40	34.73
AFRP_S 2	17.96	2.22	125.96	36.00
AFRP_S 3	22.50	2.33	137.69	45.67
Average	17.38	2.01	130.02	38.80
SD	4.44	0.38	5.43	4.89
AFRP_R1	16.85	2.04	88.28	31.13
AFRP_R2	16.10	2.81	101.11	55.05
AFRP_R3	15.40	2.40	91.13	39.90
Average	16.12	2.42	93.51	42.03
SD	0.53	0.37	17.47	9.97

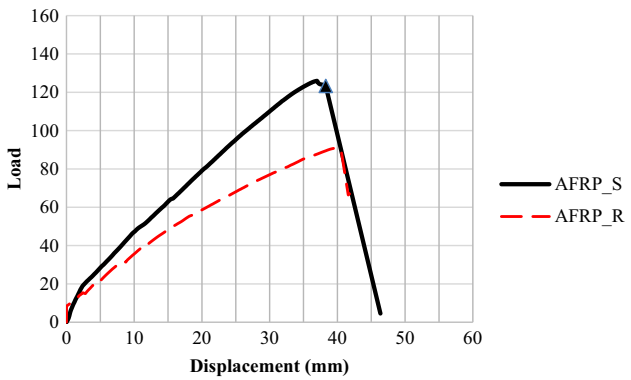

Fig. 7 Flexural test graph of AFRP_S and AFRP_R beams

Table 3, and load–displacement graphs representing this group are given in Fig. 7.

While the first cracking zone of the concrete in steel-reinforced beams is unclear, in the test of AFRP-reinforced beam with 18 ± 2 kN load and 2.42 mm deflection, it was noted that the first crack started from the beam flexural zone and the first deflection zone in the slope is seen in Fig. 8. Afterward, the flexural load-mid zone displacement graph in AFRP-reinforced beams increased linearly and the AFRP_R-reinforced beams were defeated by crushing the beam compression block in flexural and straining of AFRP_S-reinforced beams without shearing. Load-bearing capacity of AFRP_S-reinforced beam is 38% more than AFRP_R, xx% less than steel-reinforced beam.

3.3 BFRP-Reinforced Beam Results

The test data of BFRP-reinforced beams with sand-coated surface (BFRP_S) and BFRP-reinforced beams with ribbed surface (BFRP_R) are given in Table 4, and load–displacement graphs representing BFRP-reinforced beams are given in Fig. 9.

It is observed that the maximum load-bearing capacities of the beams are 109.03 kN for BFRP_S and 96.93 kN for BFRP_R. Thus, it has been determined that BFRP_S can carry %12.49 more load than BFRP_R. When the flexural load in BFRP_S beams reached an average of 18.08 kN, the concrete of the beam cracked and a deflection of 2.13 mm occurred at the midpoint of the beam. When the flexural load in BFRP_R beams reached an average of 14.18 kN, the beam concrete cracked and a 2.08 mm deflection occurred at the midpoint of the beam. The concrete cracked in the lower region of the beam and the stiffness of the beams decreased after the concrete cracked. After the first crack in the lower region of the beam, the load–deflection graph showed a

Fig. 8 Deformations of AFRP_S and AFRP_R-reinforced beams after flexural test

Table 4 BFRP-reinforced beam test results

Beam	Concrete cracking		Maximum	
	Load (kN)	Displacement (mm)	Load (kN)	Displacement (mm)
BFRP_S 1	17.85	1.95	101.22	32.32
BFRP_S 2	17.92	2.30	129.54	45.43
BFRP_S 3	18.45	2.13	109.03	40.00
Average	18.08	2.13	113.26	39.25
SD	0.27	0.14	11.94	5.38
BFRP_R1	14.69	1.98	90.17	37.61
BFRP_R2	14.13	2.26	96.87	50.97
BFRP_R3	13.73	2.00	105.74	66.59
Average	14.18	2.08	97.59	51.72
SD	0.39	0.13	6.38	11.84

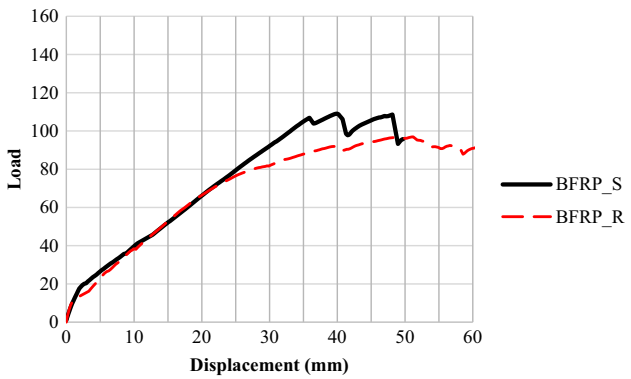

Fig. 9 Flexural test graph of BFRP_S and BFRP_R beams

linear increase, and after the critical load, the beams suddenly lost their strength (Fig. 10).

All of the BFRP-reinforced beams collapsed with shear fracture from the shear zone following flexural crack propagation in the mid-beam region.

3.4 CFRP-Reinforced Beam Results

The test results of CFRP-reinforced beams with sand-coated surface (CFRP_S) and CFRP-reinforced beams with ribbed surface (CFRP_R) are given in Table 5, and load–displacement graphs representing CFRP-reinforced beams are given in Fig. 11.

The maximum load carrying capacity of CFRP_S was found to be 153.54 kN and 109.26 kN for CFRP_R. According to the results obtained, CFRP_S beams carry 40.5% more load than CFRP_R beams. In BFRP_S beams, when the flexural load reached 18.08 kN on average, the beam concrete cracked and a deflection of 2.13 mm occurred at the midpoint of the beam. In CFRP_S beams, when the flexural load reached 20.94 kN on average, the beam concrete cracked and a deflection of 2.29 mm occurred at the midpoint of the beam. In CFRP_R beams, when the flexural load reached 14.91 kN on average, the beam concrete cracked and 1.73 mm deflection occurred at the midpoint of the beam. In the flexural test, the concrete cracked in the lower region of the beam and the stiffness of the beams decreased after the concrete cracked. After the first crack in the concrete in the lower region of the beam, the load–deflection graph showed a linear increase and the beams suddenly lost their strength after the critical load (Fig. 12).

3.5 GFRP-Reinforced Beam Results

The results of GFRP-reinforced beams with sand-coated surface (GFRP_S) and GFRP-reinforced beams with ribbed

Fig. 10 BFRP_S and BFRP_R-reinforced beam deformations after flexural test

Table 5 CFRP-reinforced beam test results

Beam	Cocnrete Cracking		Maximum	
	Load (kN)	Displacement (mm)	Load (kN)	Displacement (mm)
CFRP_S 1	20.94	2.26	153.54	26.87
CFRP_S 2	20.88	2.29	152.06	26.67
CFRP_S 3	20.99	2.33	117.32	19.03
Average	20.94	2.29	140.97	24.19
SD	0.04	0.03	16.74	3.65
CFRP_R1	15.59	1.49	97.76	24.66
CFRP_R2	13.58	1.56	107.19	22.69
CFRP_R3	15.57	2.14	137.58	37.45
Average	14.91	1.73	114.17	28.27
SD	0.94	0.29	16.99	6.54

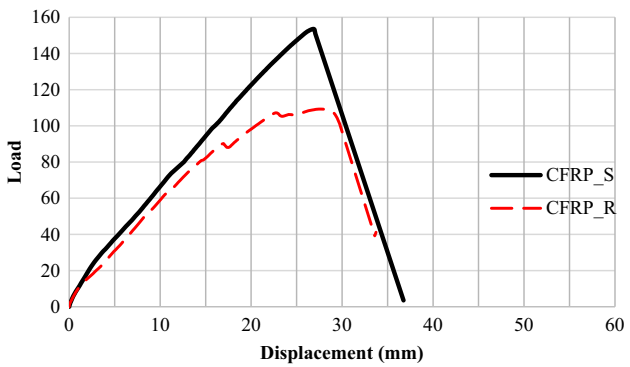

Fig. 11 Flexural test graph of CFRP_S and CFRP_R beams

surface (GFRP_R) are given in Table 6, and a comparison of their graphs is given in Fig. 13.

It is seen that the maximum load-carrying capacities of the beams are 100.07 kN for GFRP_S, 106.27 kN for GFRP_R and GFRP_R carries 5.83% more load than GFRP_R. When the flexural load in GFRP_S beams reached an average of 16.96 kN, the concrete cracked and a deflection of 1.95 mm occurred. When the GFRP_R beams reached 10.86 kN, 1.15 mm deflection occurred (Fig. 14).

4 Comparison of Results According to FRP Bar Surface Type

The results of the experiments were evaluated separately for sand-coated and ribbed beams considering load, toughness, stiffness and ductility values, respectively.

4.1 Comparison of Flexural Loads

The average maximum load value of steel-reinforced beams is 113.5 kN, and the highest load-bearing capacity is in CFRP_S beams. When the beams produced with sandy surface reinforcements are ordered from largest to smallest, they are CFRP_S 140.97, AFRP_S 130.02, BFRP_S 113.26 and GFRP_S 101.49 kN. When the beams produced with ribbed surface reinforcement are ordered from largest to smallest, they are CFRP_R 114.17, BFRP_R 97.59, AFRP_R 93.51 and GFRP_R 93.13 kN. According to the results, CFRP_R beams have the highest load carrying capacity. The test results of steel- and FRP-reinforced beams for both surface types are given in Fig. 15. The failure of the beams was in the form of shear failure after flexural. Longitudinal reinforcement fracture was not observed in FRP-reinforced beams. The flexural strength of FRP-reinforced beams increased depending on the tensile stiffness of the FRP reinforcement. There was a significant decrease in flexural stiffness due to the initial concrete tensile cracking at a flexural load of about 20 kN in aramite, basalt glass

Fig. 12 Deformations of CFRP_S and CFRP_R-reinforced beams after

Table 6 GFRP-reinforced beam test results

Beam	Concrete cracking		Maximum	
	Load (kN)	Displacement (mm)	Load (kN)	Displacement (mm)
GFRP_S 1	17.12	1.92	100.07	32.17
GFRP_S 2	15.89	1.94	92.37	28.78
GFRP_S 3	17.87	1.98	112.03	40.88
Average	16.96	1.95	101.49	33.94
SD	0.82	0.02	8.09	5.10
GFRP_R1	10.98	1.02	106.27	62.15
GFRP_R2	10.75	1.28	82.58	33.17
GFRP_R3	–	–	90.55	46.92
Average	10.86	1.15	93.13	47.42
SD	0.12	0.13	11.85	14.50

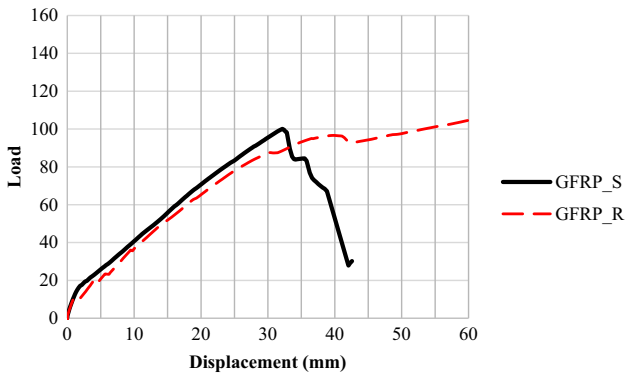

Fig. 13 Flexural test graph of GFRP_S and GFRP_R beams

FRP-reinforced beams, while it was more uncertain in carbon-reinforced beams.

4.2 Toughness Comparison

The maximum toughness value of steel-reinforced beams is 4989.42 kN.mm. The toughness values of beams reinforced with AFRP_S, CFRP_S, GFRP_S and BFRP_S on sandy surface were found to be 3128.60, 2980.40, 1922.84 and 1219.38 kN.mm, respectively. AFRP_S-reinforced beams showed the best results in terms of toughness after steel reinforcement. The toughness values of beams reinforced with BFRP_R, CFRP_R, GFRP_R and AFRP_R on ribbed surface were found to be 4036.89, 1733.02, 1620.98 and 948.82 kN.mm, respectively. According to the results, it is seen that BFRP_R has the highest toughness after steel. The test results of steel- and FRP-reinforced beams for both surfaces are given in Fig. 16.

4.3 Stiffness Comparison

The maximum stiffness value of steel-reinforced beams is 9.19 kN/mm. When the beams produced with sandy surface reinforcements are ordered from largest to smallest, CFRP_S 6.34, AFRP_S 3.76, GFRP_S 3.66 and BFRP_S 3.17 kN/mm. Thus, CFRP_S has the highest stiffness after steel. When the beams produced with ribbed surface reinforcement are ordered from largest to smallest, it is seen that CFRP_R 5.90, BFRP_R 3.42, GFRP_R 3.36 and AFRP_R 2.68 kN/mm. According to the results, CFRP_R beams have the highest stiffness after steel-reinforced beams. The stiffness values of steel- and FRP-reinforced beams according to both surfaces are given in Fig. 17.

4.4 Ductility Comparison

Ductility values of steel- and FRP-reinforced beams are given in Fig. 18. The maximum stiffness value of steel

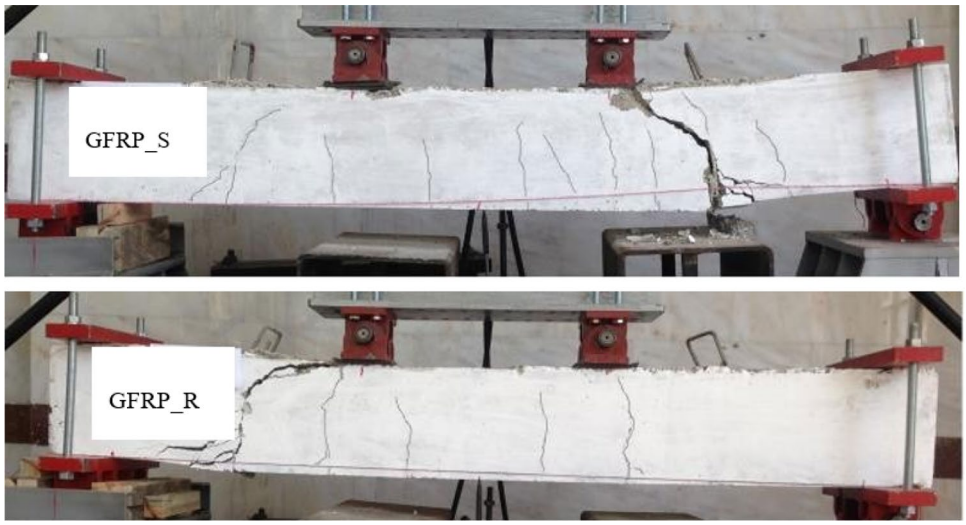

Fig. 14 Deformations of GFRP_S and GFRP_R-reinforced beams after flexural test

reinforced beams is 9.20. When the beams produced with sand-coated surface reinforcement are ordered from largest to smallest, they are BFRP_S 1.50, GFRP_S 1.43, CFRP_S 1.42 and AFRP_S 1.34, respectively. Considering these results, the highest ductility was achieved in BFRP_S beams after steel-reinforced beams. When the beams produced with ribbed surface reinforcement are ordered from largest to smallest, they are BFRP_R 3.92, GFRP_R 2.35, CFRP_R 2.12 and AFRP_R 1.15, respectively. According to the results, BFRP_R has the highest ductility after steel.

5 Conclusion and Recommendations

In the experimental study with steel- and FRP-reinforced beams, the effects of FRP reinforcement types and reinforcement surfaces on the flexural strength of the beams were investigated. All the results obtained were evaluated according to the steel-reinforced beam and each other.

Flexural and shear reinforcement of steel-reinforced beams are designed with steel reinforcement. In FRP-reinforced beams, shear reinforcement was designed with GFRP stirrups and longitudinal reinforcement was designed with different FRP reinforcements. The research results are valid only for the tested beam dimensions and with the considered reinforcement ratios. The findings are summarized below. For steel-reinforced beams, concrete damage occurred in the flexural zone and a significant ductile behavior was observed. The failure of all steel-reinforced beams occurred in the flexural zone. However, since FRP does not have yielding behavior, a yield plateau did not occur in FRP-reinforced beams. The failure of FRP-reinforced beams varies depending on the type of FRP used and the surface properties and FRP tensile stiffness. The stiffness of CFRP-reinforced beams with the highest tensile stiffness approached that of steel-reinforced beams. In addition, the tensile stiffness of FRP increased the beam flexural strength. As the flexural stiffness of the FRPs decreased, the beams displaced more at a lower load, but the failure shifted into the shear zone. Therefore, no longitudinal reinforcement damage occurred in any of the FRP-reinforced beams. Damages in FRP-reinforced beams shear damage occurred in the flexural region depending on the FRP type and surface properties.

Considering the load carried, GFRP_R carried 20%, AFRP_R 20%, BFRP_R 16%, BFRP_S 3%, CFRP_R 2% less, AFRP_S 11%, CFRP_S 21% more load compared to the steel reinforcement.

Considering the toughness, GFRP_R 71%, AFRP_R 69%, CFRP_R 62%, GFRP_S 53%, BFRP_R 52%, CFRP_S 51%, BFRP_S 48%, AFRP_S 16% have less toughness than steel reinforcement.

Considering the stiffness, it was seen that AFRP_R 70%, BFRP_S 65%, GFRP_R 63%, BFRP_R 63%, GFRP_S 62%, AFRP_S 58%, CFRP_R 40%, CFRP_S 31% less stiffness than steel reinforcement.

Considering the ductility, they have AFRP_R 84%, CFRP_S 83%, GFRP_S 82%, BFRP_S 81%, AFRP_S 78%, CFRP_R 78%, GFRP_R 76%, BFRP_R 66% less ductility than steel reinforcement.

In addition, it was concluded that FRP bars with ribbed surfaces have higher load carrying capacity and toughness than sand-coated ones.

In further studies on the use of FRP bars in beams, hybrid-reinforced beams can be investigated in order to reduce the brittleness disadvantage of FRP in reinforced concrete beams. Different combination and optimization experimental studies can be carried out to increase ductility, using both steel and FRP bars in the same reinforced concrete beam.

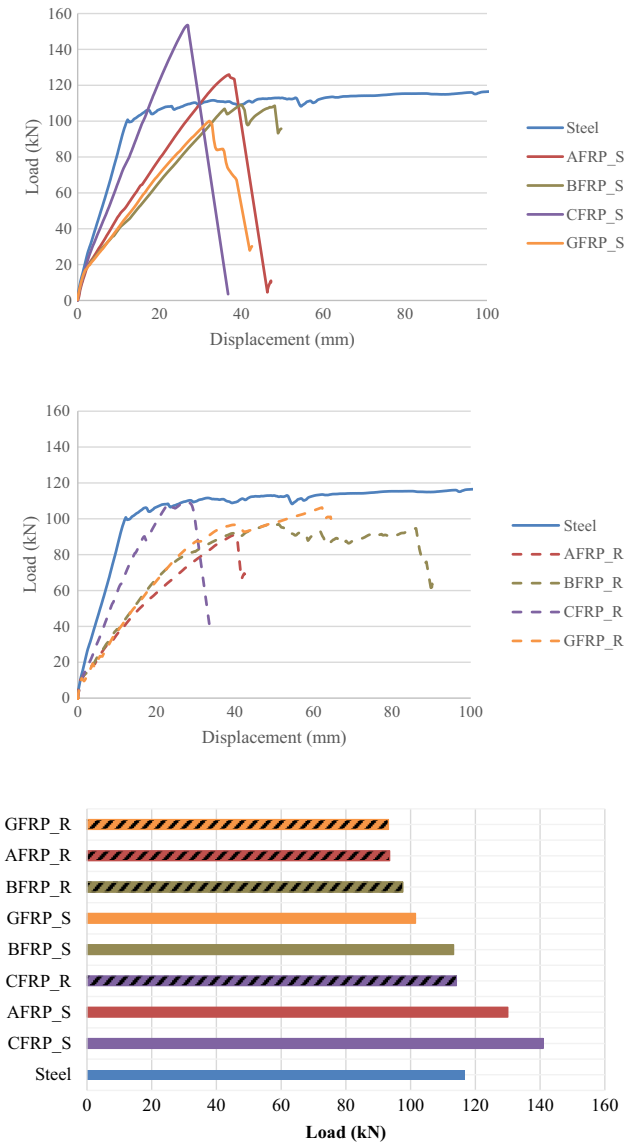

Fig. 15 FRP-reinforced beam load displacement graph with steel and sand-coated-ribbed surface

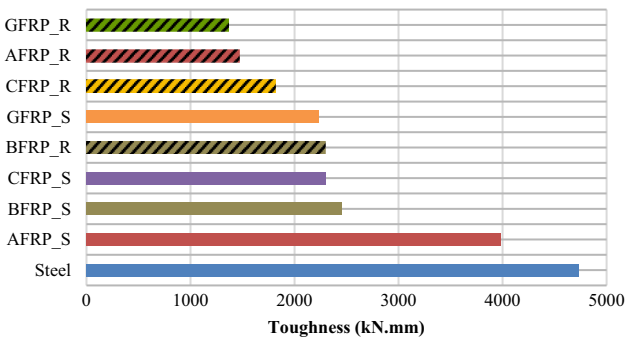

Fig. 16 Toughness values of FRP-reinforced beams with steel and sand-coated-ribbed surface

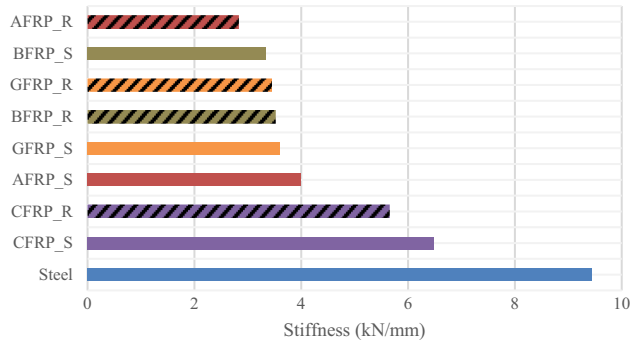

Fig. 17 Stiffness values of steel and FRP-reinforced beams with sand-coated-ribbed surface

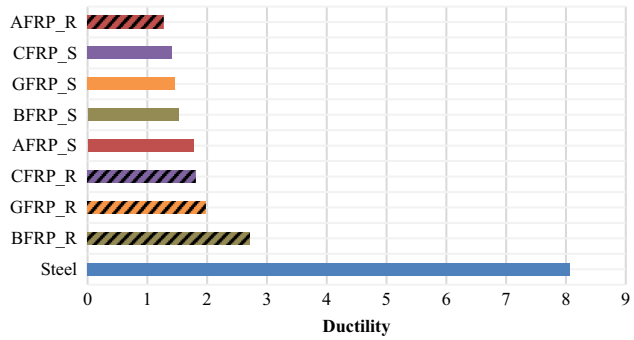

Fig. 18 Ductility values of steel and FRP-reinforced beams with sand-coated-ribbed surface

References

Abushanab A, Alnahhal W (2021) Numerical parametric investigation on the moment redistribution of basalt FRC continuous beams with basalt FRP bars. Compos Struct 277:114618. https://doi.org/10.1016/J.COMPSTRUCT.2021.114618

Abushanab A, Alnahhal W, Farraj M (2021) Structural performance and moment redistribution of basalt FRC continuous beams reinforced with basalt FRP bars. Eng Struct 240:112390. https://doi.org/10.1016/J.ENGSTRUCT.2021.112390

Al-Hamrani A, Alnahhal W (2021) Shear behavior of basalt FRC beams reinforced with basalt FRP bars and glass FRP stirrups: experimental and analytical investigations. Eng Struct 242:112612. https://doi.org/10.1016/J.ENGSTRUCT.2021.112612

Atutis E, Atutis M, Budvytis M, Valivonis J (2017) serviceability and shear response of RC beams prestressed with a various types of FRP bars. Proc Eng 172:60–67. https://doi.org/10.1016/J.PROENG.2017.02.017

Aydin F (2016) Effects of various temperatures on the mechanical strength of GFRP box profiles. Constr Build Mater 127:843–849. https://doi.org/10.1016/J.CONBUILDMAT.2016.09.130

Aydin F (2018) Experimental investigation of thermal expansion and concrete strength effects on FRP bars behavior embedded in concrete. Constr Build Mater 163:1–8. https://doi.org/10.1016/J.CONBUILDMAT.2017.12.101

Aydın F (2019) Experimental study on the flexural behaviour of a novel concrete filled hybrid beams reinforced with GFRP and steel bars.

KSCE J Civ Eng 23(11):4710–4717. https://doi.org/10.1007/S12205-019-1714-6/METRICS

Aydın F, Arslan Ş (2021) Investigation of the durability performance of FRP bars in different environmental conditions. Adv Concr Constr 12(4):295–302. https://doi.org/10.12989/acc.2021.12.4.295

Aydın E, Boru E, Aydın F (2021) Effects of FRP bar type and fiber reinforced concrete on the flexural behavior of hybrid beams. Constr Build Mater 279:122407. https://doi.org/10.1016/J.CONBUILDMAT.2021.122407

Brózda K, Selejdak J, Koteš P (2017) The analysis of beam reinforced with FRP bars in bending. Proc Eng 192:64–68. https://doi.org/10.1016/j.proeng.2017.06.011

Chen H, Yi WJ, Ma ZJ, Hwang HJ (2020) Modeling of shear mechanisms and strength of concrete deep beams reinforced with FRP bars. Compos Struct 234(October 2019):111715. https://doi.org/10.1016/j.compstruct.2019.111715

Deifalla A (2015) Torsional behavior of rectangular and flanged concrete beams with FRP reinforcements. J Struct Eng 141(12):04015068. https://doi.org/10.1061/(ASCE)ST.1943-541X.0001322

Deifalla A (2022) Punching shear strength and deformation for FRP-reinforced concrete slabs without shear reinforcements. Case Stud Constr Mater 16:e00925. https://doi.org/10.1016/J.CSCM.2022.E00925

Deifalla A, Salem NM (2022) A machine learning model for torsion strength of externally bonded FRP-reinforced concrete beams. Polymers 14(9):1824. https://doi.org/10.3390/POLYM14091824

Deifalla A, Khalil MS, Abdelrahman A (2014) simplified model for the torsional strength of concrete beams with GFRP stirrups. J Compos Constr 19(1):04014032. https://doi.org/10.1061/(ASCE)CC.1943-5614.0000498

Dhahir MK, Ammash HK, Nadir W, Nasr MS (2021) An efficiency factor for the bottle shaped concrete strut in deep beams reinforced with longitudinal FRPs bars. Mater Today: Proc 42:2050–2057. https://doi.org/10.1016/j.matpr.2020.12.258

Dong HL, Zhou W, Wang Z (2019) Flexural performance of concrete beams reinforced with FRP bars grouted in corrugated sleeves. Compos Struct 215:49–59. https://doi.org/10.1016/J.COMPSTRUCT.2019.02.052

Ebid AM, Deifalla A (2021) Prediction of shear strength of FRP reinforced beams with and without stirrups using (GP) technique. Ain Shams Eng J 12(3):2493–2510. https://doi.org/10.1016/J.ASEJ.2021.02.006

Fan X, Zhou Z, Wenlin Tu, Zhang M (2021) Shear behaviour of inorganic polymer concrete beams reinforced with basalt FRP bars and stirrups. Compos Struct 255:112901. https://doi.org/10.1016/J.COMPSTRUCT.2020.112901

Gao D, Zhang C (2020) Shear strength calculating model of FRP bar reinforced concrete beams without stirrups. Eng Struct 221:111025. https://doi.org/10.1016/J.ENGSTRUCT.2020.111025

Ge W, Ashour AF, Cao D, Weigang Lu, Gao P, Jiamin Yu, Ji X, Cai C (2019) Experimental study on flexural behavior of ECC-concrete composite beams reinforced with FRP bars. Compos Struct 208:454–465. https://doi.org/10.1016/J.COMPSTRUCT.2018.10.026

Gravina RJ, Smith ST (2008) Flexural behaviour of indeterminate concrete beams reinforced with FRP bars. Eng Struct 30(9):2370–2380. https://doi.org/10.1016/j.engstruct.2007.12.019

Han S, Zhou Ao, Jinping Ou (2021) Relationships between interfacial behavior and flexural performance of hybrid steel-FRP composite bars reinforced seawater sea-sand concrete beams. Compos Struct 277:114672. https://doi.org/10.1016/J.COMPSTRUCT.2021.114672

Hassan MM, Deifalla A (2016) Evaluating the new CAN/CSA-S806-12 torsion provisions for concrete beams with FRP reinforcements. Mater Struct 49(7):2715–2729. https://doi.org/10.1617/S11527-015-0680-9/FIGURES/13

Huang Z, Chen W, Tran TT, Pham TM, Hao H, Chen Z, Elchalakani M (2021) Experimental and Numerical study on concrete beams reinforced with basalt FRP bars under static and impact loads. Compos Struct 263:113648. https://doi.org/10.1016/J.COMPSTRUCT.2021.113648

Jafarzadeh H, Nematzadeh M (2020) Evaluation of post-heating flexural behavior of steel fiber-reinforced high-strength concrete beams reinforced with frp bars: experimental and analytical results. Eng Struct 225(March):111292. https://doi.org/10.1016/j.engstruct.2020.111292

Johnson J, Man Xu, Jacques E (2021) Predicting the self-centering behavior of hybrid FRP-steel reinforced concrete beams under blast loading. Eng Struct 247:113117. https://doi.org/10.1016/J.ENGSTRUCT.2021.113117

Li C, Zhu H, Niu G, Cheng S, Zhiqiang G, Yang L (2022) Flexural Behavior and a new model for flexural design of concrete beams hybridly reinforced by continuous FRP bars and discrete steel fibers. Structures 38(2021):949–60. https://doi.org/10.1016/j.istruc.2022.02.037

Liu Xi, Sun Y, Tao Wu, Liu Y (2020) Flexural Cracks in steel fiber-reinforced lightweight aggregate concrete beams reinforced with FRP bars. Compos Struct 253:112752. https://doi.org/10.1016/J.COMPSTRUCT.2020.112752

Mehany S, Mohamed HM, El-Safty A, Benmokrane B (2022) Bond-Dependent coefficient and cracking behavior of lightweight self-consolidating concrete (LWSCC) beams reinforced with glass- and basalt-FRP bars. Constr Build Mater 329:127130. https://doi.org/10.1016/J.CONBUILDMAT.2022.127130

Qin W, Liu X, Xi Z, Huang Z, Al-Mansour A, Fernand M (2021) Experimental research on the progressive collapse resistance of concrete beam-column sub-assemblages reinforced with steel-FRP composite bar. Eng Struct 233:111776. https://doi.org/10.1016/J.ENGSTRUCT.2020.111776

Ren F, Liu T, Chen G, Xie P, Xiong MX, Yuan T, Chen Y, Guo S (2021) Flexural behavior and modelling of FRP-bar reinforced seawater sea sand concrete beams exposed to subtropical coastal environment. Constr Build Mater 309:125071. https://doi.org/10.1016/J.CONBUILDMAT.2021.125071

Salem NM, Deifalla A (2022) Evaluation of the strength of slab-column connections with FRPs using machine learning algorithms. Polymers 14(8):1517. https://doi.org/10.3390/POLYM14081517

Sogut K, Dirar S, Theofanous M, Faramarzi A, Nayak AN (2021) Effect of transverse and longitudinal reinforcement ratios on the behaviour of RC T-beams shear-strengthened with embedded FRP bars. Compos Struct 262:113622. https://doi.org/10.1016/J.COMPSTRUCT.2021.113622

Sokairge H, Elgabbas F, Elshafie H (2022) Structural behavior of RC beams strengthened with prestressed near surface mounted technique using basalt FRP bars. Eng Struct 250:113489. https://doi.org/10.1016/J.ENGSTRUCT.2021.113489

Su C, Wang X, Ding L, Chen Z, Liu S, Zhishen Wu (2021) Experimental study on the seismic Behavior of seawater sea sand concrete beams reinforced with steel-FRP composite bars. Eng Struct 248:113269. https://doi.org/10.1016/J.ENGSTRUCT.2021.113269

Sun Z, Linchen Fu, Feng DC, Vatuloka AR, Wei Y, Gang Wu (2019) Experimental Study on the flexural behavior of concrete beams reinforced with bundled hybrid steel/FRP bars. Eng Struct 197:109443. https://doi.org/10.1016/J.ENGSTRUCT.2019.109443

TS 500 (2000) Design and Construction Rules of Reinforced Concrete Structures. Turkish Standards Institute, Ankara

Xiao SH, Lin JX, Li LJ, Guo YC, Zeng JJ, Xie ZH, Wei FF, Li M (2021) Experimental Study on flexural behavior of concrete beam

reinforced with GFRP and steel-fiber composite bars. J Build Eng 43:103087. https://doi.org/10.1016/J.JOBE.2021.103087

Yang Y, Pan D, Gang Wu, Cao D (2021) A new design method of the equivalent stress-strain relationship for hybrid (FRP bar and steel bar) reinforced concrete beams. Compos Struct 270(March):114099. https://doi.org/10.1016/j.compstruct.2021.114099

Yasmin M, Tarawneh A, Arar F, Al-Zu'bi A, Al-Ghwairi A, Al-Jaafreh A, Tarawneh M (2021) Flexural strength prediction for concrete beams reinforced with FRP bars using gene expression programming. Structures 33(June):3163–72. https://doi.org/10.1016/j.istruc.2021.06.045

Zhang Y, Elsayed M, Zhang LV, Nehdi ML (2021) Flexural behavior of reinforced concrete t-section beams strengthened by NSM FRP bars. Eng Struct 233:111922. https://doi.org/10.1016/J.ENGSTRUCT.2021.111922

Zhou Y, Gao H, Zhiheng Hu, Qiu Y, Guo M, Huang X, Biao Hu (2021) Ductile, durable, and reliable alternative to FRP bars for reinforcing seawater sea-sand recycled concrete beams: steel/FRP composite bars. Constr Build Mater 269:121264. https://doi.org/10.1016/J.CONBUILDMAT.2020.121264

Zhu H, Cheng S, Gao D, Neaz SM, Li C (2018) Flexural behavior of partially fiber-reinforced high-strength concrete beams reinforced with FRP bars. Constr Build Mater 161:587–597. https://doi.org/10.1016/J.CONBUILDMAT.2017.12.003